

# Quantum Dots Are Powerful Multipurpose Vital Labeling Agents in Zebrafish Embryos

Sandra Rieger,<sup>1</sup> Rajan P. Kulkarni,<sup>2</sup> Dan Darcy,<sup>2†</sup> Scott E. Fraser,<sup>2</sup> and Reinhard W. Köster<sup>1\*</sup>

Recently, inorganic fluorescent contrast agents composed of semiconductor materials have been introduced to biological imaging approaches. These so-called quantum dots provide unique and promising properties unreached by organic fluorophores, but their use as contrast agents within live organisms has been limited, probably due in part to concerns about their *in vivo* tolerance. Using transparent zebrafish embryos, we challenged quantum dots with a series of intravital imaging problems. We show that quantum dots provide a high fluorescent yield within targeted tissues, possess immense photostability, can be targeted to specific subcellular compartments, remain within targeted cells as lineage tracers, are easily separable from conventional organic fluorescent dyes, and are fixable, allowing them to be used in combination with immunohistochemistry after live recordings. Thus, quantum dots combine the specific advantages of different organic fluorescent contrast agents and promise to become the first fluorophore feasible for long-lasting intravital time-lapse studies. Finally, we show by colabeling blood vessels of the vasculature and major axon tracts of the nervous system that, for establishing these networks, the same guidance cues might be used in some body parts, whereas in others, both networks appear to develop independently from one another. Thus, the bright fluorescence of quantum dots will help to unravel many open questions in the fields of embryology, cell biology, as well as phenotyping and disease diagnosis. *Developmental Dynamics* 234:670–681, 2005. © 2005 Wiley-Liss, Inc.

**Key words:** zebrafish; bio-imaging; quantum dots; microangiography; contrast agent; lineage tracer

Received 9 February 2005; Revised 22 April 2005; Accepted 16 June 2005

## INTRODUCTION

The ever-continuing demand for intravital contrast agents of different and brighter colors, reduced size, more stability, less toxicity, and greater versatility has led recently to the establishment of so-called quantum dots as biological labeling agents. Of these semiconductor nanocrystals, cadmium selenide quantum dots have been most commonly used for biological applica-

tions. Because crystal size alone determines the excitation and emission characteristics, a crayon box of fluorophores can be generated with a single synthesis strategy (Bruchez et al., 1998; Jaiswal et al., 2003). Also, appropriate masking and coupling chemistry has only to be developed once. Different coats using zinc sulfide (Mattoussi et al., 2001), silica (Bruchez et al., 1998; Chan and Nie, 1998), or micelles (Dubertret et al.,

2002; Wu et al., 2003) have been developed to increase the fluorescence of the quantum dots and to render them soluble in aqueous medium. Such quantum dots have been found to be nontoxic in cultured cells (Jaiswal et al., 2003), within the mouse vasculature (Larson et al., 2003), in *Xenopus* embryos (Dubertret et al., 2002), and in tumor cells injected into mice embryos (Voura et al., 2004). Adapter molecules at-

The Supplementary Material referred to in this article can be accessed at [www.interscience.wiley.com/jpages/1058-8388/suppmat](http://www.interscience.wiley.com/jpages/1058-8388/suppmat)

<sup>1</sup>GSF - National Research Center for Environment and Health, Institute of Developmental Genetics, Neuherberg-Munich, Germany

<sup>2</sup>Biological Imaging Center, Beckman Institute (139-74), California Institute of Technology, Pasadena, California

Grant sponsor: Caltech Biological Imaging Center; Grant sponsor: the German Bundesministerium für Bildung und Forschung; Grant number: Biofuture-Award 0311889.

<sup>†</sup>Dr. Darcy's present address is University of California San Diego, Division of Biology, San Diego, CA.

\*Correspondence to: Reinhard W. Köster, GSF-National Research Center for Environment and Health, Institute of Developmental Genetics, 85764 Neuherberg, Munich, Germany. E-mail: [reinhard.koester@gsf.de](mailto:reinhard.koester@gsf.de)

DOI 10.1002/dvdy.20524

Published online 18 August 2005 in Wiley InterScience ([www.interscience.wiley.com](http://www.interscience.wiley.com)).

tached to the outer shells can further functionalize quantum dots for specific recognition and binding of distinct proteins (Jaiswal et al., 2004), making them suitable for use as diagnostic agents (Gao et al., 2004).

The range of applications for quantum dots as biological labeling agents as well as understanding their specific advantages and limits in living specimen has just begun to be explored. The lack of attention toward quantum dots by researchers in the intravital imaging field may be based on concerns regarding the potential toxicity of semiconductor materials, questioning the longevity of their protective surface coat. Due to its optical clarity, external development, and ease of manipulation, the zebrafish is perhaps the most suited vertebrate model organism for imaging embryogenesis. Morphogenetic tissue movements, cellular interactions, and behaviors, and even subcellular dynamics can be observed at high resolution within the living organism (Henry et al., 2000; Köster and Fraser, 2001a; Niell et al., 2004). Surprisingly, the use of quantum dots as a vital labeling agent has not been explored in zebrafish embryos to date. We show that quantum dots can be injected into zebrafish embryos in large amounts with no harm to embryogenesis over several days. Furthermore, their superior spectral properties in live and fixed specimens make quantum dots a powerful analytical agent that can be used in combination with numerous available green fluorescent protein (GFP) -transgenic zebrafish lines. Their easy employment as lineage tracer or bright microangiography agent broadens their applicability in living embryos and promises that quantum dots will become a routine intravital labeling agent for analyzing many aspects of embryogenesis within the living and developing organism.

## RESULTS

### Quantum Dots Provide a Bright Vital Label in Zebrafish Embryos

Quantum dots have been used for many *in vitro* applications, but proba-

bly based on the assumption that semiconductor materials are toxic, few *in vivo* approaches using quantum dots as a vital labeling agent have been reported so far. Thus, we tested streptavidin-conjugated QD605 quantum dots (Quantum Dot Corporation) that consist of a core of cadmium selenide surrounded by a zinc sulfide shell enhancing the quantum yield for brighter fluorescence (<http://www.qdots.com/live/render/content.asp?id=71>) in zebrafish embryos. A secondary outer coat provides a hydrophilic surface and attachment sites for streptavidin, rendering these dots soluble for *in vivo* applications such as cytoplasmic microinjection.

To test whether zebrafish embryos tolerate these quantum dots during embryogenesis, we injected a bolus (100 nM, 1.7 nl) of QD605 into the cytoplasm of one of the two blastomeres at the two-cell stage. Excitation with blue light resulted in a bright red fluorescent signal emitted by the descendants of the injected cell at the eight-cell stage (Fig. 1A). The quantum dots appeared to spread through cytoplasmic bridges that connect all zebrafish blastomeres during the first cleavage stages (Kane, 1999; Fig. 1A). The injected embryos developed indistinguishably from uninjected counterparts, showing a bright fluorescence throughout the embryo during gastrulation (Fig. 1B) and somitogenesis stages (Fig. 1C). Even during organogenesis, red fluorescence derived from the injected quantum dots could be observed throughout the body (Fig. 1D).

In some tissues of the embryo, clusters of quantum dots were found (Fig. 1D, black arrowheads), possibly caused by a tendency of the QD605 to form small aggregates. These aggregates could also be found when aqueous dilutions of QD605 were dispersed on a coverslip and imaged by confocal laser scanning microscopy (Fig. 1E, see yellow arrowheads). Sonication of the quantum dots for 5 min before injection dissolved the aggregates (Fig. 1F). When sonicated quantum dots were injected at the one-cell stage, zebrafish embryos developed properly with intense red fluorescence throughout tissues of all germ layers, indicating that sonication neither destroys

the quantum dots nor releases toxic contents from quantum dots (Fig. 1H).

To evaluate a tolerable QD605 dose, zebrafish embryos were injected with sonicated quantum dots at varying concentrations. Up to  $10^8$  quantum dots could be injected with most embryos showing no malformations or developmental problems during embryogenesis, similar to injection results that are usually obtained with mRNA or plasmid DNA. Further increase of the injection concentration resulted in elevated levels of malformations and embryonic death (Fig. 1G).

### Emission Properties of Quantum Dots Remain Unaffected by the Cellular Environment

One of the characteristics of quantum dots is their narrow emission band, separated by a large Stoke's shift from the excitation wavelength. This feature allows an easy separation of excitation and emission signals and offers the simultaneous detection of multiple nonoverlapping quantum dot colors (Bruchez et al., 1998; Jaiswal et al., 2003; Voura et al., 2004).

To investigate whether these emission characteristics are influenced by their surrounding environment *in vivo*, the emission spectra of QD605 were compared in water (Fig. 2A), phosphate buffer (Fig. 2B), and intravitaly in zebrafish embryos (Fig. 2C) using laser scanning confocal microscopy combined with liquid crystal tunable filters for spectroscopy (Lansford et al., 2001). As observed *in vitro*, intracellular QD605 show an emission maximum at 605 nm. Also, the narrow emission profile of approximately 60 nm in width, ranging from approximately 580 nm to 640 nm, remains unaltered when compared with QD605 spectra obtained *in vitro*. This stability indicates that the intracellular environment of zebrafish embryonic cells does not affect the characteristic emission properties of QD605.

### Subcellular Localization of Quantum Dots Can Be Regulated by Different Coats

Quantum dots coated with trimethoxysilylpropyl urea and acetate groups bind with high affinity components in

the nucleus (Bruchez et al., 1998). Also, quantum dots that had been encapsulated by micelles using reagents that are applied in lipofection strategies have been reported to preferentially accumulate in the nucleus in *Xenopus* embryonic cells (Dubertret et al., 2002). In contrast, streptavidin-conjugated QD605 injected at the one-cell stage into zebrafish embryos appeared to be excluded from the nucleus. When imaged in the embryonic eye at higher magnification using laser scanning confocal microscopy, the quantum dots appeared to outline the cellular morphology of lens fiber and retinal cells (Fig. 2F). Thus, we compared their cellular fluorescence with vital fluorescent labels of defined localization.

Bodipy Ceramide labels the extracellular matrix and cell membranes, but its signal obtained from embryonic zebrafish eyes appeared to be more restricted than QD605 (compare Fig. 2D with F). In contrast, mRNA injection of a nuclear localized histone 2B fusion protein to monomeric red fluorescent protein (mRFP; Campbell et al., 2002) labeled the bean-shaped nuclei within lens fiber and retinal cells, resembling the unlabeled structures in QD605-containing cells (compare Fig. 2G with F). Finally, injections of mRNA encoding the fusion protein *unc76:GFP* (Dynes and Ngai, 1998),

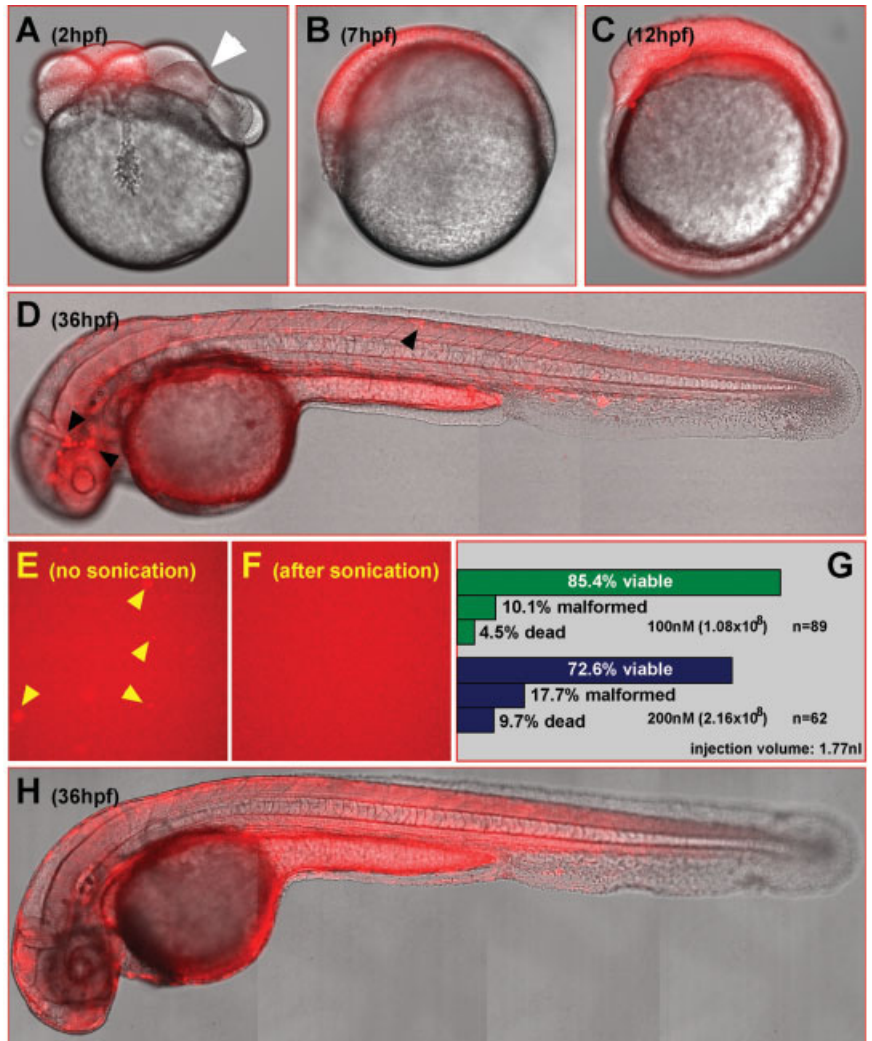


Fig. 1.

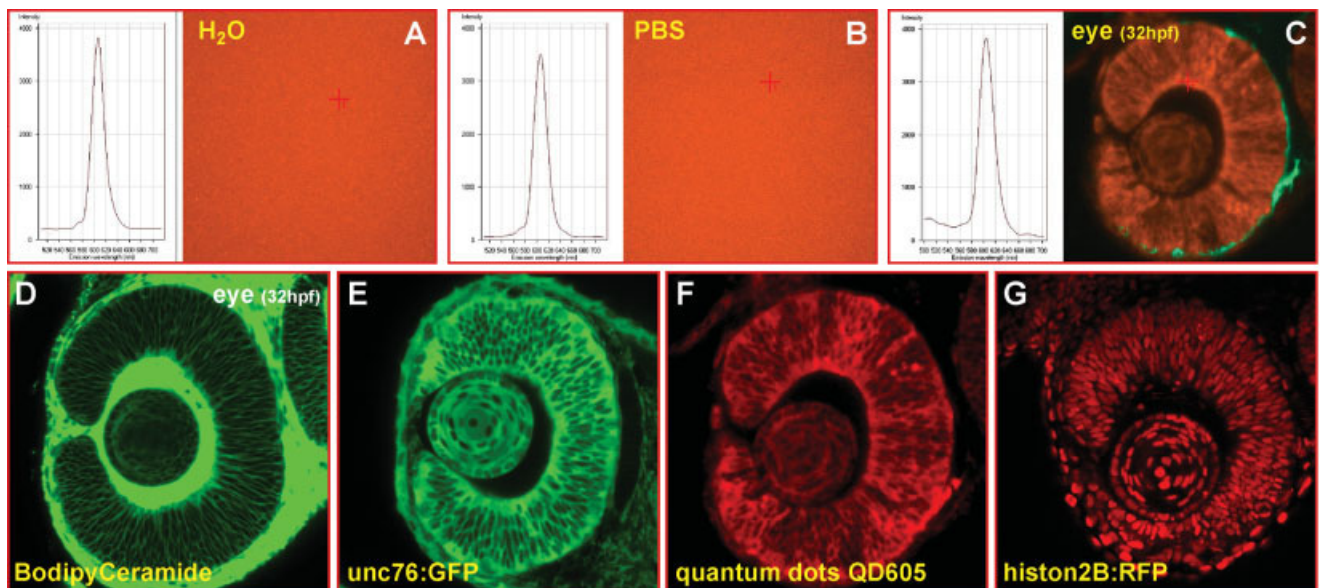


Fig. 2.

which labels the cytoplasm but is excluded from the nucleus, appeared to result in a very similar fluorescent label of lens fiber and retinal cells in the zebrafish embryonic eye as QD605, copying their cellular localization (compare Fig. 2E with F). This finding suggests that streptavidin-conjugated QD605 localize to the cytoplasm and are excluded from the nucleus and indicates that, by using differently tailored coats, quantum dots can be localized to distinct cellular compartments.

**Fig. 1.** Quantum dots provide bright vital labeling during zebrafish embryogenesis. A–D: Lateral views of embryo injected with QD605 (100 mM, 1.7 nI) at the two-cell stage. A–D: Bright red fluorescent labeling can be observed during the first cleavage stages (A, weaker labeling of descendants from the uninjected blastomere (white arrowhead) indicates spreading of the quantum dots during first cleavage stages), gastrulation (B), somitogenesis (C), and organogenesis (D) without affecting embryonic development. E: The tendency of QD605 to form aggregates (aqueous QD605 dispersion on a coverslip, see yellow arrowheads for aggregates) results in bright fluorescent clusters in some tissues (D, arrowheads). F, H: These aggregates can be dissolved by sonication (F, sonicated aqueous QD605 dispersion on coverslip) before embryonic injection, resulting in evenly labeled embryos (H). G: Whereas  $10^8$  injected quantum dots are being tolerated by developing zebrafish embryos, higher injection amounts appear to interfere with embryogenesis. hpf, hours postfertilization.

**Fig. 2.** Emission and localization properties of QD605. A–C: Comparison of the emission spectra of QD605 measured in water (A), phosphate buffered saline (PBS, B), and within retinal cells of zebrafish embryos (C) indicates that the QD605 emission spectra remain unaltered in vitro and in vivo irrespective of their environment. Spectroscopy was performed using laser scanning confocal microscopy combined with liquid crystal tunable filters (LSM510 Meta system, Zeiss). The cross hair demarcates the spot from which the spectra were obtained. Relocating the cross hair to different points of fluorescence did not affect the emission spectra significantly. D–G: Comparison of differently localized cellular fluorescent labels within lens fiber and retinal cells in developing zebrafish eyes using laser scanning confocal microscopy; whereas the membrane-localized dye Bodipy Ceramide (D) and the nuclear-localized histon2B-mRFP fusion protein (G) result in a different vital cellular label, the signal obtained from streptavidin-conjugated QD605 (F) appeared to resemble very closely the labeling of the unc76:GFP fusion protein, which labels the cellular cytoplasm but is excluded from the nucleus (E). hpf, hours postfertilization; RFP, red fluorescent protein.

## Quantum Dots as Lineage Tracer in Zebrafish Embryos

To test whether streptavidin-conjugated QD605 can be used to reliably mark descendants of injected cells, QD605 were coinjected with mRNA encoding GFP, an established lineage tracer in zebrafish embryos, into individual blastomeres at the 32- and 64-cell stage. At this developmental stage, the cytoplasmic connections between embryonic blastomeres have ceased to exist (Kane, 1999). The successful restriction of the injection to a subset of blastomeres can be ensured right after the injection using a fluorescence stereomicroscope to detect the red fluorescence of the QD605 (Fig. 3A,B).

At 30% epiboly, a cluster of approximately 20 cells close to the animal pole displayed strong red fluorescence emitted by the QD605 (Fig. 3C,D). The same cells also emitted a green fluorescent signal derived from the translated GFP (Fig. 3E) as the overlay of both fluorescent signals showed a perfect match (Fig. 3F). This finding indicates that QD605 had been passed to the daughter cells of the initially injected blastomeres through rounds of cell division. As the quantum dots had not been able to spread any further, these results show that streptavidin-conjugated QD605 cannot pass through gap junctions in zebrafish embryonic cells.

After onset of gastrulation, the cluster of fluorescent cells dispersed, likely due to extensive movements and relocation of gastrulating cells (Fig. 3G). Whereas most cells still displayed fluorescence of both QD605 (Fig. 3H) and GFP (Fig. 3I), some of the cells appeared to display GFP fluorescence only (Fig. 3J, white arrowheads). This finding could be caused by the tendency of QD605 to form aggregates unlike GFP, thereby being passed on to only one of the daughter cells during a cell division. In contrast, cells emitting QD605 fluorescence independently of the GFP signal could not be found. These coinjection results show that streptavidin-conjugated QD605 quantum dots reliably mark descendants of individually injected cells in zebrafish embryos and can be used as lineage tracer. One has to bear in mind though that the finally

labeled cell population may not represent the entire but rather a large subtraction of the descendants.

## Quantum Dot Labeling to Follow Cell Dynamics and Changes in Morphology

To directly address the potential of quantum dot labeling for following individual cells and their dynamic behavior during embryonic development, zebrafish embryos were injected at the one-cell stage with mRNA encoding a nuclear localized histone 2B-EGFP fusion protein. Subsequently, individual blastomeres were injected at the 64-cell stage with QD605. This approach resulted in a green fluorescent labeling of the nuclei of nearly every cell during gastrulation stages, with a few cells being colabeled in their cytoplasm with red fluorescent quantum dots. Such QD605-marked cells were followed by time-lapse imaging over several hours during gastrulation (Fig. 3K–R).

The cytoplasmic quantum dot fluorescence was able to reveal the contact and release of individual cells during gastrulation (Fig. 3K–P, yellow arrow). This contact release occurred past several other cells (Fig. 3N), as judged by the number of interspersed labeled nuclei. Subsequently, the chromatin in one of the cells condensed (Fig. 3O, white arrow) followed by the division of the double-fluorescent cell, with both emerging daughter cells carrying the red fluorescence of the QD605 label in their cytoplasm (Fig. 3Q,R white arrows).

To address whether more elaborate cell morphology can be visualized using quantum dots, a skin cell from a similarly injected embryo was imaged at high magnification at 36 hours postfertilization (hpf; Fig. 3T). In addition, individual notochord cells were injected with QD605. Their bright fluorescence revealed the polygonal shape of differentiated notochord cells with the nucleus and vacuoles being spared by the quantum dots. Thus, quantum dots, when being used as lineage tracers, can reveal dynamic changes in morphology and cell behavior during embryonic development, with image recording at high magnification displaying the morphology of individual cells.

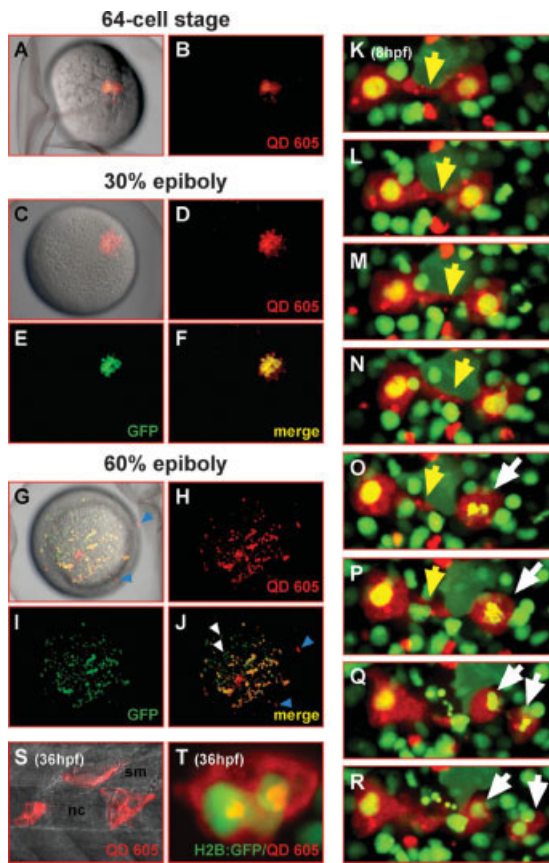


Fig. 3.

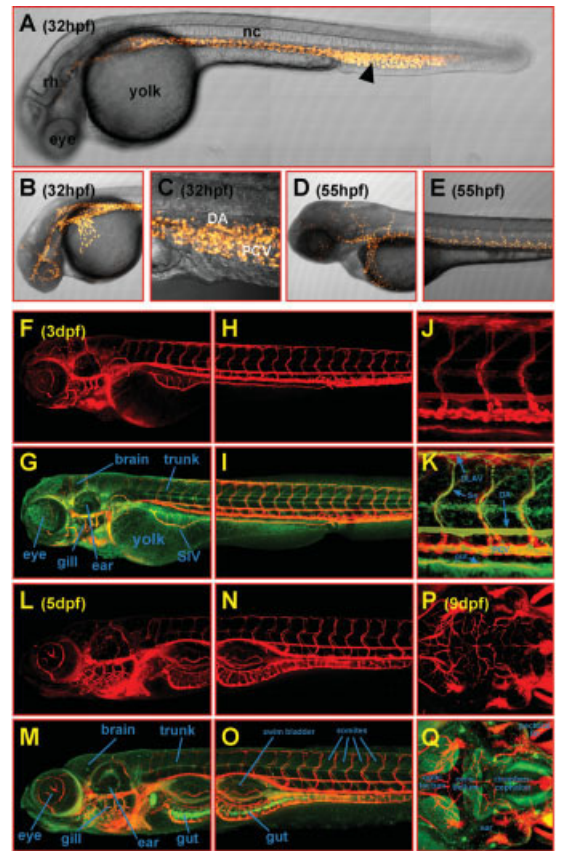


Fig. 4.

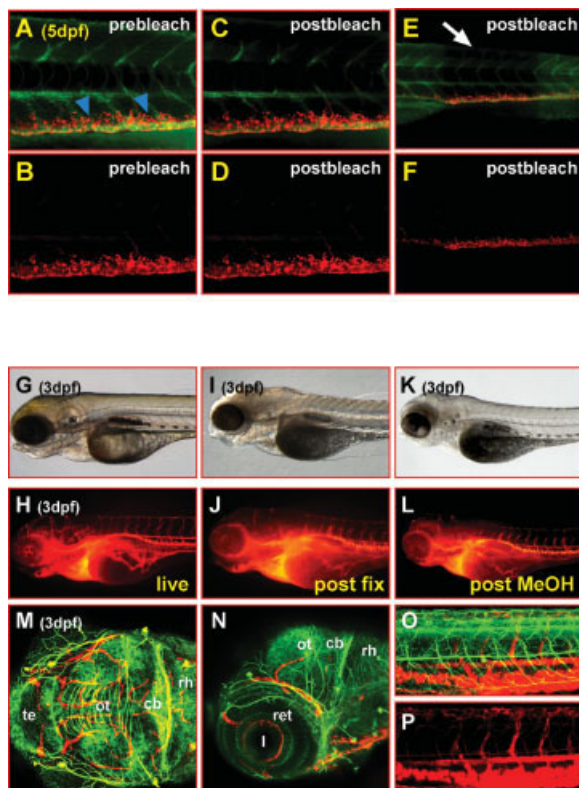


Fig. 5.

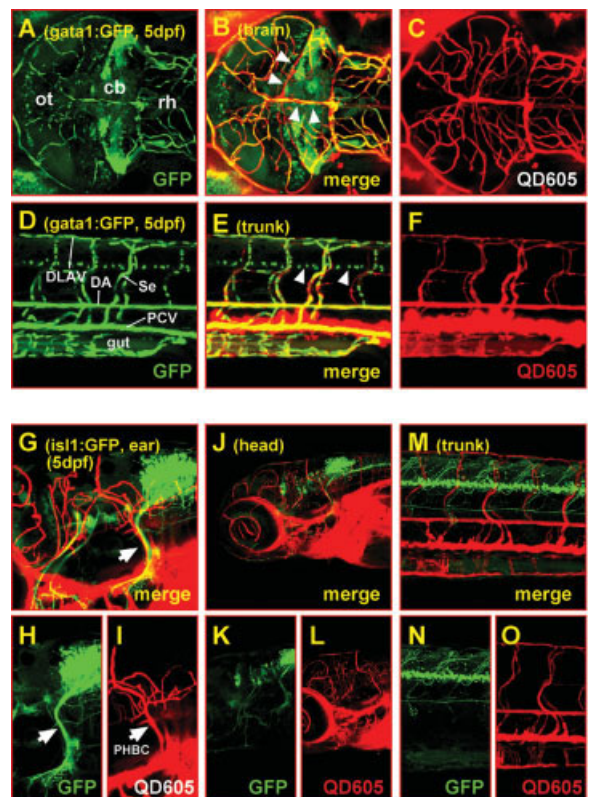


Fig. 6.

**Fig. 3.** Lineage tracing of zebrafish embryonic cells using QD605. **A:** Two blastomeres of a zebrafish embryo at the 64-cell stage (overlay of transmitted light image with QD605 fluorescence) have been co-injected with QD605 and mRNA encoding green fluorescent protein (GFP), an established lineage tracer in zebrafish embryos. **B:** The restriction to two individual blastomeres can be observed immediately after the injection by the red fluorescence of QD605 using a fluorescence stereomicroscope. **C–E:** At 30% epiboly (C, overlay of transmitted light image with QD605 fluorescence), green fluorescence emitted by the meanwhile translated GFP can be observed (E) in addition to the red QD605-derived fluorescence (D). Both fluorescent signals are localized to a single continuous cell cluster of approximately 20 cells close to the apical pole of the embryos. **F:** The overlay of both fluorescent channels shows that both signals overlap completely. This finding indicates that streptavidin-conjugated QD605 do not spread to neighboring cells through gap junctions but are being passed on to descendants of the initially injected blastomeres through rounds of cell divisions. **G:** At 60% epiboly, the single cell cluster of fluorescent cells has dispersed, likely due to extensive cell movements of gastrulating cells. **H,I:** Red QD605-derived fluorescence (H) and green GFP-emitted fluorescence (I) can still be detected in numerous cells. **J:** The overlap of both fluorescent channels shows that most fluorescent cells co-emit GFP and QD605 fluorescence, indicating that streptavidin-conjugated QD605 can be used to mark descendants of individually injected cells. Some cells appear to display green GFP fluorescence only (J, white arrowheads). The lack of QD605 in this subfraction of cells may be caused by QD605 being propagated to only one daughter cell during a round of cell division, due to their tendency to form aggregates. **G,J:** A few red fluorescent signals emitted from QD605 that do not co-emit GFP fluorescence appear to be derived from quantum dots that are not localized within the embryo, perhaps being deposited between the embryo and the chorion during the injection procedure (compare blue arrowheads in J and G). These results show that streptavidin-conjugated QD605 can be used as lineage tracers in zebrafish embryos to label the vast majority of descendants from an injected individual precursor cell. **K–R:** To directly follow individual cell dynamics, zebrafish embryos were injected with mRNA (150 ng/ $\mu$ l) encoding a histone2B–EGFP fusion protein at the single-cell stage followed by QD605 injection of an individual blastomere at the 64-cell stage. **H:** As such labeled cells disperse during gastrulation individually QD605-labeled cells could be followed by time-lapse recording using laser scanning confocal microscopy. Starting at 8 hours postfertilization (hpf) stacks of images spaced by 5  $\mu$ m, respectively, were recorded every 5 min covering an optical section of 30  $\mu$ m in total. A sequence from a several-hours recording is displayed with images from a 10- $\mu$ m fraction of the recorded stacks being projected into single frames by maximum intensity projection. Two cells making and releasing contact (K–P, yellow arrowheads) while undergoing morphological changes can be observed due to the QD605-derived fluorescence of their cytoplasm. Subsequently, the chromatin of one of the labeled cells condenses (O,P, white arrows), and two daughter cells (Q,R, white arrows) arise from a cell division, each carrying the QD605 label. **T:** To record more elaborate cell morphology, a skin cell from a similarly injected embryo was imaged at 36 hpf. **S:** In addition, individual notochord cells were injected at 36 hpf with QD605. Pictures from a recorded stack of images (60  $\mu$ m at 1  $\mu$ m distance) were projected by maximum intensity projection into a single plane. Due to the bright fluorescent labeling, the polygonal shape of the notochord cell can be appreciated with the nucleus and vacuoles being spared by the fluorescent quantum dots. nc, notochord; sm, somitic muscle.

**Fig. 4.** Quantum dot microangiography. Living zebrafish embryos of progressing developmental stages were injected into the heart ventricle with a 1  $\mu$ M suspension of streptavidin-conjugated QD605 to label the vasculature by virtue of the blood flow carrying the quantum dots through the entire vascular network. Subsequently, laser scanning confocal microscopy was used to record the distribution of the quantum dots. **A:** Lateral view of a 32 hours postfertilization (hpf) embryo; the vasculature is quite primitive, consisting mainly of a major artery and vein running below the notochord (nc). **B,C:** Injected QD605 attach in clusters to the vascular endothelium (B, maximum intensity projection of 100 sections each 3  $\mu$ m apart, see also Movie 1 for motility of attached QD605) and accumulate in reticular cells (A, arrowhead; C, maximum intensity projection of 61 sections each 2.5  $\mu$ m apart). **D,E:** These deposited QD605 might serve during ongoing embryogenesis as a source to label the endothelium of newly forming blood vessels (55 hpf, D, maximum intensity projection of 100 sections each 3  $\mu$ m apart; E, maximum intensity projection of 85 sections each 2  $\mu$ m apart). **F–K:** At 3 days postfertilization (dpf; F–K, lateral views), the vasculature is by far more elaborate, forming a dense network in the head (F,G, maximum intensity projection of 71 sections each 5  $\mu$ m apart) and trunk (H,I, maximum intensity projection of 71 sections each 3  $\mu$ m apart). G,I,K: Counterstaining with Bodipy Ceramide was used to visualize the morphological context. **L–O:** At 5 dpf (L–O, lateral views), the gills (L,M, maximum intensity projection of 51 sections each 5  $\mu$ m apart) and intestinal region (N,O, maximum intensity projection of 115 sections each 2  $\mu$ m apart) have acquired a branched vascular network. M,O,Q: Bodipy Ceramide counterstaining. **P,Q:** Finally, at 9 dpf (dorsal views, maximum intensity projection of 122 sections each 2  $\mu$ m apart) the vasculature interweaving the midbrain hindbrain region was imaged deep to the ventral brain area. For three-dimensional animations of the vasculature at 3, 5, and 9 dpf, see also Movies 2–4. SIV, subintestinal vein.

**Fig. 5.** Streptavidin-conjugated QD605 are extremely photostable in vivo and withstand fixation for immunohistochemical analyses. **A–F:** Lateral views of the trunk of a 5-day-old zebrafish larva that has been soaked overnight in Bodipy Ceramide (green fluorescence) and was subsequently subjected to QD605 microangiography (red fluorescence). Bodipy Ceramide fluorescence in the trunk muscles and notochord diminishes after 150 consecutive 488-nm laser scans (7.9 sec each) of 3.75 mW (compare A and C), whereas the QD605 fluorescence of the reticular cells remains unaltered (compare B and D). E,F: Thus, at lower magnification, an area with bleached Bodipy Ceramide labeling can be observed (E) when compared with adjacent tissue, whereas the strength of the QD605 fluorescence appears equally strong throughout the trunk (F, see also Supplementary Movie 5 for bleaching dynamics). **G–L:** Lateral views of the head of a 3-day-old zebrafish larva that has been subjected to streptavidin-conjugated QD605 microangiography; strong labeling of the vasculature can be observed in the living specimen (G,H) that remains after fixation overnight in 4% paraformaldehyde in phosphate buffered saline containing 0.1% Tween 20 (I,J) and appears still unaffected after storage in methanol at  $-20^{\circ}\text{C}$  and subsequent rehydration (K,L). **M–P:** Such embryos were subsequently subjected to immunohistochemistry using an antibody against acetylated tubulin to mark axon tracts of differentiating neurons in the brain (M, dorsal view, maximum intensity projection of 49 sections each 2  $\mu$ m apart; N, lateral view, maximum intensity projection of 29 sections each 2  $\mu$ m apart; images were recorded using the Meta channel of a Zeiss LSM510 laser scanning microscope, fluorescence was recorded from 499 to 670 nm in steps of 10.7-nm intervals, the emission of both fluorophores was subsequently separated by linear unmixing) and the trunk (O, lateral view, maximum intensity projection of 57 sections each 2  $\mu$ m apart; P, QD605 emission only, to highlight the blood vessel network within the trunk; images were recorded using the Meta channel of a Zeiss LSM510 laser scanning microscope, fluorescence was recorded from 499–670 nm in steps of 10.7-nm intervals, the emission of both fluorophores was subsequently separated by linear unmixing) for double-labeling purposes. This finding shows that blood vessels obey the segmented pattern of the brain and trunk. cb, cerebellum; l, lens; ot, optic tectum; ret, retina; rh, rhombencephalon; te, telencephalon; dpf, days postfertilization.

**Fig. 6.** Combining green fluorescent protein (GFP) and quantum dot fluorescence in living specimens. **A–C:** Maximum intensity projection of 82 sections each 1.97  $\mu$ m apart; dorsal views of the midbrain and anterior hindbrain of a 5-day-old homozygous *gata1:GFP* (strain 781) zebrafish larvae. Laser scanning confocal microscopy with excitation at 488 nm reveals both green fluorescent blood vessels and cell clusters in the brain due to GFP expression in erythrocytes and distinct neuronal populations (see also Movie 6 for their three-dimensional organization). C: The vasculature also displays an intense red fluorescence due to quantum dots carried along with the blood serum. B: Note that the signal from the neuronal clusters does not appear in the red channel and is not double stained in the merged image, indicating that there is no bleeding of the GFP fluorescence into the red channel. Thus, both fluorescent signals can be separated using conventional filter sets. **D–F:** In the lateral views of the trunk of the same specimen, all the characteristic blood vessels can be detected by both GFP (D) and quantum dot (F) fluorescence, demonstrating that both fluorophores can be efficiently separated when colocalized within the same structure (note the exclusively green signal of GFP-expressing cells in the ventral neural tube, white arrowheads in E). **G–O:** Projections of image stacks recorded by laser scanning confocal microscopy. Lateral views of heterozygous 5-day-old *islet1:GFP* zebrafish larvae after QD605 microangiography. The GFP-expressing vagus sensory ganglion (H, white arrow) and the primordial hindbrain channel (I, white arrow) appear to share a common trajectory (G, maximum intensity projection of 35 sections each 1.97  $\mu$ m apart) also verified by three-dimensional re-sectioning. This coprojection does not appear to be characteristic for the majority of axon tracts (K) and blood vessels (L) in the brain (J, maximum intensity projection of 100 sections each 3.03  $\mu$ m apart) and trunk (M–O, maximum intensity projection of 49 sections each 1.98  $\mu$ m apart), respectively. cb, cerebellum; DA, dorsal aorta; DLAV, dorsal longitudinal anastomotic vessel; ot, optic tectum; PCV, posterior cardinal vein; PHBC, primordial hindbrain channel; rh, rhombencephalon; Se, intersegmental vessel; dpf, days postfertilization.

## Quantum Dots Are a Powerful Microangiography Contrast Agent

Understanding the development and function of the cardiovascular system is one of the most pressing research areas to date, but its *in vivo* accessibility is limited. Zebrafish embryos, with their transparency, external development, and ease of manipulation allow the development of the cardiovascular system to be followed and influenced directly *in vivo* (Isogai et al., 2001; Hove et al., 2003).

Microangiography (Weinstein et al., 1995) was attempted by injecting pulses of 1  $\mu$ M QD605 suspension in water into the ventricle of the zebrafish embryonic heart at 32 hpf. The quantum dots were immediately carried away with the blood stream, resulting in a bright fluorescent labeling of the entire vasculature, which is quite simple at this developmental stage (Fig. 4A).

Soon after the intracardial injection, quantum dots began to accumulate, probably through phagocytosis within the reticular cells of the trunk and tail (Fig. 4B,C) that line the dorsal aorta and posterior cardinal vein. Nevertheless, not all of the quantum dots were cleared from the blood stream, and some selected cells of the vascular endothelium deposited the quantum dots as clusters on their outer membranes (Fig. 4B). High-speed laser-scanning microscopy of a part of the primordial hindbrain channel (PHBC), a vein just posterior to the otic vesicle, revealed that these quantum dot clusters were not stationary but could move along the endothelial wall, probably providing a source of quantum dots for further labeling of blood vessels (see Supplementary Movie 1, which is available at [www.interscience.wiley.com/jpages/1058-8388/suppmat](http://www.interscience.wiley.com/jpages/1058-8388/suppmat)). When the injected embryos were continued to be raised, newly formed blood vessels were outlined by such quantum dot clusters on their endothelial wall (compare Fig. 4B,C with D,E), thereby documenting the embryonic pattern of vasculogenesis.

## Quantum Dot Microangiography in Zebrafish Larvae

The bright labeling of the zebrafish embryonic vasculature by quantum dots prompted us to investigate whether embryos at older stages re-

quiring increasing imaging depths are still accessible for microangiography. First, 3-day-old anesthetized larvae were subjected to QD605 injection into the beating left heart ventricle. Immediately, the entire vasculature of the head and trunk was fluorescently labeled (Fig. 4F,H, see also three-dimensional [3D] animation in Supplementary Movie 2), revealing the progression in vasculogenesis that has occurred from 32 hpf until 3 days of development (e.g., compare Fig. 4B with F). Counterstaining with Bodipy Ceramide allowed placing the blood vessels into the context of the larval body plan (Fig. 4G,I). In addition to a more complex brain vasculature, the gills have already formed at 3 days postfertilization (dpf). Also, the segmented nature of the trunk vasculature with the repetitive pattern of dorsoventral running intersegmental vessels (Fig. 4H,I; see also higher magnification in Fig. 4J,K) has matured. At this stage, the vasculature surrounding the developing gut appears to form on top of the yolk (Fig. 4F,G) with the subintestinal vein already reaching the endgut of the larvae.

A further progression in vasculogenesis especially in the gills and intestinal system was found, when the quantum dot microangiography was repeated in 5-day-old larvae (Fig. 4L,N, see also 3D animation in Supplementary Movie 3). Whereas the gills showed a much more elaborated vascular network (Fig. 4L,M), the gut, which becomes motile for food transport by 4 days, is now surrounded by a mesh of vasculature (Fig. 4N,O), likely required for the efficient transport of resorbed nutrients.

Finally, we attempted to image the vasculature of the mid- and hindbrain region in 9-day-old larvae (Fig. 4P). Bodipy Ceramide most intensely labels the neuropil in the brain (Fig. 4Q), thereby providing anatomical landmarks for orientation. The brightness of the quantum dots provides a high photon yield that allows even blood vessels positioned in very ventral aspects of the brain to be visualized by laser scanning confocal microscopy in living specimens (see also 3D animation in Supplementary Movie 4). Such vital labeling could be potentially useful for addressing blood vessel innervation of early aggressive

brain tumors such as medulloblastoma or to analyze the ability of fluorescent compounds to cross the blood-brain barrier.

## Quantum Dots Are Photostable *In Vivo*

Organic fluorophores, when scanned repeatedly, are subject to photochemical reactions leading eventually to the destruction of their fluorescent properties. Compared with typical fluorophores used in immunohistochemistry, quantum dots as inorganic nanocrystals appear to be far more stable during long-term light exposure in solution or fixed cell cultures (Jaiswal et al., 2003; Wu et al., 2003). Therefore, we set out to compare the photostability of streptavidin-conjugated QD605 to a vital fluorescent label of considerable photostability, Bodipy Ceramide, commonly used in living zebrafish embryos (Cooper et al., 1999). After overnight exposure to Bodipy Ceramide, 5-day-old zebrafish larvae were subjected to microangiography using QD605, which were subsequently allowed to settle in reticular cells of the trunk (Fig. 5A, blue arrowheads). The trunk of these double-labeled larvae was heavily exposed to 488-nm laser light by 150 consecutive scans of 7.9 sec at 3.73 mW. With the exception of the blood serum, all Bodipy Ceramide labeling in stationary tissues, such as the trunk muscles and notochord cells, faded almost completely (Fig. 5C, compare to A, see also time course of bleaching in Supplementary Movie 5). This resulted in a dark square in the zebrafish trunk containing almost no Bodipy Ceramide labeling when compared with adjacent tissues at lower magnification (Fig. 5E, white arrow). In contrast, the fluorescent signal of the quantum dots appeared unaffected, showing a similar strength before and after repetitive high power laser scanning (compare Fig. 5C,D). Thus, the reticular cells in the ventral trunk remained fluorescently labeled in a continuous stripe of strong, even fluorescence along their anteroposterior distribution (Fig. 5F). This finding indicates that the immense photostability of quantum dots is independent of the environment within the living zebrafish larvae. Furthermore, as the fluorescence yield of the quantum dots does not increase with the ongoing photode-

struction of Bodipy Ceramide, quenching of the quantum dot fluorescence signal by the presence of another fluorophore appears to be unlikely.

### Streptavidin-Conjugated Quantum Dots Combined With Immunohistochemistry

Most vital fluorescent labels bear the disadvantage of escaping fixation and, thus, are incompatible with immunohistochemical protocols. To test whether streptavidin-conjugated QD605 remain within the labeled tissue and survive fixation, quantum dot microangiography was performed on 3-day-old embryos, resulting in bright labeling of their elaborated vascular network (Fig. 5G,H). After fixing the embryos overnight at 4°C in 4% paraformaldehyde, the quantum dots still marked the entire vasculature of the embryos with nearly no loss of the fluorescent signal (Fig. 5I,J). When subsequently transferred to methanol and rehydrated after several days, embryos still displayed the characteristic quantum dot fluorescence with high tissue specificity (Fig. 5K,L).

As these results promised that quantum dot-labeled embryos could be used for further immunohistochemical double labeling approaches, zebrafish embryos were subjected to antibody staining after microangiography, fixation and methanol treatment, using an antibody against acetylated tubulin. This antibody detects differentiating neurons and, thus, reveals the extensive axonal and dendritic network of the emerging zebrafish nervous system (Wilson et al., 1990). Using laser scanning confocal microscopy, both the axon tracts of the midbrain and cerebellum could be analyzed in detail in parallel to the vasculature, providing these brain areas with oxygen and nutrients (Fig. 5M,N). Also in the trunk, the pattern of the vasculature and motoneurons reflecting the segmented organization of the neural tube could be displayed in relation to one another (Fig. 5O,P). Bearing in mind the range of colors and coupling methods available for quantum dots, these fluorescent semiconductor crystals promise to make feasible numerous multicolor labeling approaches.

### Separating Quantum Dot Fluorescence From GFP Expression

Due to their transparency, external development, and accessibility for genetic manipulations, zebrafish embryos are especially suited for intravital imaging approaches using the genetically encoded GFP. A continuously growing number of GFP-expressing stable transgenic zebrafish lines is being produced, and recent advances in transposon insertion techniques have increased the number of such GFP lines manifold (Kawakami et al., 2004; Parinov et al., 2004). As the emission profile of GFP is quite broad, reaching into red wavelengths, separation of the respective emission signals of GFP and red fluorophores in colabeled specimens can be difficult.

Quantum dots are excited at wavelengths suitable for coexcitation of GFP, thus minimizing the amount of excitation light required compared with dual excitation of conventional fluorophores. This feature results in greatly reduced phototoxicity effects. The large Stoke's shift of quantum dot-emitted fluorescence should allow GFP and quantum dot fluorescence to be separated and detected easily. To test this assumption, we used two different stable transgenic GFP-expressing zebrafish lines and subjected their embryos to streptavidin-conjugated QD605 microangiography at 5 dpf.

First, embryos of the strain 781 expressing GFP under the control of the *gata1*-enhancer were used (Long et al., 1997). In this line, GFP is expressed in circulating blood cells, but also ectopically in various cell types of the central nervous system, including the retina, optic tectum, and cerebellum (Fig. 6A). After microangiography, transgenic *gata1*:GFP larvae were imaged with a confocal microscope using a single laser line at 488 nm. In addition to the green GFP fluorescence in neuronal cell clusters of the brain, these larvae displayed an intensely labeled brain vasculature due to the strong red fluorescence of the quantum dots (Fig. 6C). Both emission signals could be easily separated with standard filter sets, showing that most blood vessels in the larval brain either run along rostrocaudal or mediolateral boundaries,

such as the dorsal midline or the midbrain–hindbrain boundary (Fig. 6B, white arrowheads), with most vessels respecting the compartmentation of the brain by remaining on the ipsilateral side within the optic tectum or hindbrain (see also 3D animation in Supplementary Movie 6).

To investigate whether the fluorescent emission signals can be separated efficiently within the same structure, we turned to the repetitive, simpler vasculature of the trunk. GFP-expressing erythrocytes could be visualized throughout the characteristic trunk arteries and veins (Fig. 6D–F), such as the dorsal longitudinal anastomotic vessel, the intersegmental vessels, the dorsal aorta, or the posterior cardinal vein. These vessels could also be displayed by recording the fluorescence emitted by the quantum dots in the blood serum (Fig. 6F), showing a good colocalization with the GFP-expressing erythrocytes.

### Pathfinding of the Vascular and Axonal Network Appear To Be Independent

During their development, both the nervous system and the vasculature face the same challenge: to setup a complex interwoven network and to form the right connections. Thus, blood vessels and axonal tracts could share guidance signals and substrates on common highways to simplify pathfinding. Indeed, recent results obtained in mice and fish embryos have demonstrated that pathfinding axons and interconnecting endothelial cells share the use of the diffusible guidance factor Netrin1 and its receptor Unc5B (Lu et al., 2004; Park et al., 2004).

Transgenic zebrafish larvae expressing GFP under control of the *istlet1*:enhancer display an intense green fluorescence in cranial motor neurons and their axon tracts (Higashijima et al., 2000). When QD605 microangiography was performed in these larvae, it appeared that some axon tracts and blood vessels such as the vagus sensory ganglion and the PHBC just posterior to the otic vesicle share common trajectories (Fig. 6G–I, white arrows). However, other GFP-expressing axonal tracts in the brain, when examined for their alignment

with blood vessels, did not seem to coalesce with the vasculature (Fig. 6J–L), as observed in larvae stained against  $\alpha$ -tubulin expression (Fig. 5M,N). Similarly, in the trunk, the blood vessels and axon tracts with their segmented repetitive organization form individual nonoverlapping networks along both the dorsoventral and rostrocaudal axis (Fig. 6M–O). Thus, pathfinding within the vasculature and the nervous system may coalesce by sharing the use of the same directional guidance signals in some tissues, whereas in others, their pathfinding may be independent of one another, following independent routes and guidance cues.

## DISCUSSION

Recently, inorganic chemistry advances have provided fluorescent semiconductor nanocrystals of unique properties for use as contrast agents. With the development of hydrophilic coats and conjugation chemistry, these inorganic materials quickly entered the field of bioimaging and diagnosis. Here, they mostly served to replace organic dyes as fluorophores coupled to secondary antibodies commonly used in immunohistochemical techniques on fixed biological material. Despite their clear advantages such as the pronounced photostability or the large Stoke's shift and narrow bandwidth of their emitted light, quantum dots have not yet obtained significant attention as intravital labeling agents. This finding is perhaps due to concerns regarding the toxicity of semiconductor materials, such as cadmium selenide, but might also be caused by the currently small product palette that is commercially available. To encourage further product development, these inorganic contrast agents must be tested directly *in vivo* and the properties of the currently available compounds examined in detail.

By exploiting the transparency of the zebrafish embryo and its easy accessibility for *in vivo* manipulation, we showed that the unique *in vitro* spectral properties of quantum dots are being conserved *in vivo*, displaying a huge Stoke's shift of the emitted light covering only a narrow bandwidth of approximately 60 nm. This finding allows quantum dot fluores-

cence to be separated very easily from the emission of conventional organic fluorophores and GFP variants and, thus, offers many new colabeling strategies. Furthermore, red-emitting quantum dots are efficiently excited with blue light, enabling the simultaneous excitation and signal separation of quantum dots and green-emitting organic fluorophores. So far, the use of conventional red-emitting organic fluorophores required additional excitation of double-labeled samples with green light. Therefore, imaging quantum dots together with green-emitting fluorophores saves an entire excitation step and imposes far less phototoxicity to live specimens. Moreover, for simultaneous signal detection of green- and red-emitting organic fluorophores (such as the commonly used Alexa 488 and Alexa 546 in antibody or DiI/DiO double-labeling approaches), the requirement to separate green excitation (for the red-emitting fluorophore, e.g., Alexa 546, DiO) from green-emitted fluorescence (e.g., Alexa 488, DiI) by narrow filter sets can be completely neglected.

By direct delivery through cytoplasmic injection at the single cell stage, we found that quantum dots are tolerated by the zebrafish embryo at high quantities and are carried through successive developmental stages with no obvious influence upon embryogenesis over several days. The tendency of the quantum dots to aggregate could be overcome by sonicating them before injection. This aggregation behavior might not be intrinsic to quantum dots, but could be caused by the conjugated streptavidin. Recently released nonconjugated quantum dots (<http://www.qdots.com/live/index.asp>) that have been coated with polyethylene glycol to minimize interactions may prove to be more powerful for *in vivo* labeling, thereby allowing even higher quantities to be microinjected into zebrafish cells.

Our finding that quantum dots do not pass through gap junctions but remain within the injected cells renders them useful as lineage tracers with a high photon yield. Furthermore, we showed that quantum dots could be used to follow labeled cells during their developmental course to reveal cellular behavior. In addition, quantum dots could be useful to mark do-

nor cells in transplantation and tissue recombination experiments, with the quantum dots not only discriminating between host and donor cells but also revealing the morphology of the differentiated transplanted cells. As we showed that quantum dots can be easily separated from GFP fluorescence and represent a powerful colabeling strategy in stable transgenic GFP-expressing zebrafish strains, they promise to become a powerful cell lineage and cell population marker for labeling individual cells or to address fate mapping questions with respect to genetically marked GFP-expressing cell populations. This long-lasting integrity of their surface-coat together with the longevity of their photon yield makes quantum dots the first fluorophores suitable for long-term time-lapse imaging, even deep within the organism.

Furthermore, the small net charge should allow quantum dots to be applicable in electroporation and iontophoresis labeling strategies, delivering them to individual cells during organogenesis stages (Fraser, 1996; Concha et al., 2003; Teh et al., 2003). This feature could be used to study the fate and differentiation behavior, such as migration of single cells, to obtain a detailed understanding of single-cell morphology or to address projection patterns of individual neurons. As quantum dots are very efficient multiphoton fluorophores, even cells deep inside embryonic tissues should be accessible for detailed morphological analysis (Larson et al., 2003). Finally, transfecting a mixture of differently colored quantum dots could represent an alternative to the "DiOlistic" labeling approach for color-coding cells (Gan et al., 2000). In fact, mixtures of cells labeled with five different quantum dot samples of varying emission spectra have been successfully discriminated by emission-scanning multiphoton microscopy (Voura et al., 2004).

In many experiments involving live observations of cells, it is desired to subsequently relate the dynamic observation to the expression of distinct proteins, for example to identify specific cell types, to monitor the organization of subcellular components (e.g., microtubules), or to analyze a certain cell state (e.g., mitotic, apoptotic). As

many vital labeling strategies do not withstand tissue fixation protocols, such questions often pose great difficulties to the experimental design. We demonstrated that streptavidin-conjugated quantum dots remain within the labeled tissue, with their bright fluorescence surviving the fixation procedures and dehydration. Thus, quantum dots promise to better combine the large fields of *in vivo* and *in vitro* imaging, solving a long-standing problem.

Cardiovascular diseases are among the most common and life-threatening afflictions in modern industrialized countries. As zebrafish and their vascular system are accessible to genetic manipulation (Chen et al., 1996; Stainier et al., 1996) and the development of their vascular system can be followed easily due to the transparency of the embryos, vasculogenesis is one of the major research topics in the field of zebrafish developmental biology. Detailed knowledge about the progression of vascular system development has been derived from microangiography experiments, mounting in the establishment of a stage-dependent vascular atlas (Isogai et al., 2001). Previously, green fluorescent latex beads (fluoresceinated) were used to label the blood serum of zebrafish embryos and larvae (Weinstein et al., 1995). Using quantum dots, we were able to obtain a resolution of the vascular system at comparable detail, ranging from early differentiation to late larval stages. The embryos and larvae survived the quantum dot load in their blood system and could be imaged repeatedly, with the quantum dots marking newly formed vessels.

Of interest, although of different composition than latex-beads, streptavidin-conjugated quantum dots accumulate after microangiography in selective cells that line the vasculature and become especially enriched in tail reticular cells. Thus, it appears that some cells of the vascular endothelium have a tendency to bind substances carried by the blood serum. Quantum dot microangiography in transgenic zebrafish strains expressing GFP-fusion proteins under control of the *fli1*-enhancer to label different compounds of the vascular endothelium (Lawson and Weinstein, 2002), therefore,

might help better understand processes of material deposit and accumulation along vascular walls, a common cause for arteriosclerosis. Using intravital laser scanning confocal microscopy, the required intensity of a fluorescence signal for this bio-imaging approach may be ensured by the bright fluorescent emission of the quantum dots, and intolerable phototoxicity will be avoided.

Recently, molecular evidence has been presented in mouse and zebrafish that the vascular and the neuronal network share common attractive and repulsive guidance cues for establishing their connectivity, respectively (Park et al., 2003; Wang et al., 2003; Lu et al., 2004; Park et al., 2004; Torres-Vazques et al., 2004; Gitler et al., 2004; Gu et al., 2005). This finding would suggest common trajectories along which axon tracts and blood vessels project. Our finding from quantum dot double-labeling experiments that, during embryogenesis, blood vessels and axon tracts coalesce only in distinct tissues argues for local coregulation of both networks in distinct tissues through common guidance factors, but not for a global theme of neural and vascular codevelopment throughout the embryo. Thus, quantum dots offer many new strategies in the field of intravital imaging and may soon become a standard phenotype analysis and diagnosis tool in the research fields of cardiovascular development and disease.

## EXPERIMENTAL PROCEDURES

### Zebrafish Maintenance

Raising, spawning, and maintaining of zebrafish lines were performed as described previously (Westerfield, 1995; Kimmel et al., 1995).

### Injection

Zebrafish embryos were injected at the one-cell stage with 1.7 nl of a 100 nM suspension of streptavidin-conjugated Quantum Dots QD605 (Quantum Dot Corporation, Hayward, CA) in water. Sonication of the quantum dot solution to disperse aggregates was performed in a PC3 sonicator (L&R Ultrasonics, Keary, NJ) at 55

kHz for 5 min. Capped mRNA encoding cytoplasmic GFP or a nuclear localized fusion of GFP with histone 2B (Kanda et al., 1998) for coinjection with QD605 dots was synthesized from respective pCS2+ expression vectors (Rupp et al., 1994) using the SP6 mMMESSAGE mMACHINE Kit (Ambion, Inc., Austin, TX) and injected at a concentration of 150 ng/ $\mu$ l.

### Immunohistochemistry

Antibody staining was performed as described (Lyons et al., 2003) with the following modifications. Embryos were incubated with the primary (1:500 dilution of mouse anti-acetylated tubulin, Sigma) and secondary antibody (1:200 dilution of anti-mouse IgG conjugated to Alexa-Fluor 488, Molecular Probes) in phosphate buffered saline (PBS) containing 10% normal goat serum, 1% Triton X-100, and 0.1% Tween 20. Before image recording, embryos were fixed in 4% paraformaldehyde/PBS/0.1% Tween 20.

### Microangiography

For microangiography, zebrafish embryos were anesthetized in 0.01% tricaine in 30% Danieau medium and embedded on their back in 1.2% ultra-low gelling agarose (Sigma). A glass capillary filled with 1  $\mu$ M of QD605 in water was inserted into the atrium or ventricle of the beating heart. Using mild air pressure, several pulses of QD605 suspension were delivered into the pierced heart chamber with waiting intervals between each delivery to allow the heart to clear injected QD605 from the chamber through the blood stream, thereby labeling the entire vasculature. Successful labeling of the vasculature was confirmed immediately after the injection under a fluorescent stereomicroscope using a 590-nm-long pass filter. To obtain a morphological counterstain, embryos were soaked in 0.001% Bodipy Ceramide for 12 hr before quantum dot injection (Cooper et al., 1999; Köster and Fraser, 2001b).

### Intravital Imaging

Noninvasive intravital imaging was performed as described in detail (Köster and Fraser, 2005). Shortly, embryos

were anesthetized in 0.01% tricaine in 30% Danieau medium containing 0.75 mM phenylthiourea to prevent pigmentation before image recording. Still images of QD605-injected embryos were either recorded with a digital camera (Axiocam Hrc, Zeiss) on a fluorescence stereomicroscope (MZ16FA, Leica) or by laser scanning confocal microscopy (LSM510Meta, Zeiss), which was also used for recording stacks of pictures for 3D reconstruction and time-lapse recording. Subsequent image processing, projections, and animations were performed using Photoshop 6.0 (Adobe), LSM software (Zeiss) and QuickTime 6.5.1 (Apple), respectively.

## ACKNOWLEDGMENTS

We thank Aura Keeter and Petra Hammerl for excellent animal care. We thank Thomas Lisse for critically reading the manuscript. We thank all the members of our laboratories as well as the Wurst and Bally-Cuif laboratories for discussion and helpful suggestions. We also thank Shuo Lin for providing us with the transgenic zebrafish *gata1:gfp* 781-strain and Hitoshi Okamoto and Laure Bally-Cuif for supplying us with the *isl1:gfp* transgenic zebrafish line. An expression construct containing the *histon2B:mRFP* fusion was kindly provided by Sean G. Megason.

## REFERENCES

- Bruchez MJ, Moronne M, Gin P, Weiss S, Alivisatos AP. 1998. Semiconductor nanocrystals as fluorescent biological labels. *Science* 281:2013–2016.
- Campbell RE, Tour O, Palmer AE, Steinbach PA, Baird GS, Zacharias DA, Tsien RY. 2002. A monomeric red fluorescent protein. *Proc Natl Acad Sci U S A* 99:7877–7882.
- Chan WC, Nie S. 1998. Quantum dot bioconjugates for ultrasensitive nonisotopic detection. *Science* 281:2016–2018.
- Chen JN, Haffter P, Odenthal J, Vogelsang E, Brand M, van Eeden FJM, Furutani-Seiki M, Granato M, Hammerschmidt M, Heisenberg CP, Jiang YJ, Kane DA, Kelsh RN, Mullins MC, Nüsslein-Volhard C. 1996. Mutations affecting the cardiovascular system and other internal organs in zebrafish. *Development* 123:293–302.
- Concha ML, Russel C, Regan JC, Tawk M, Sidi S, Gilmour DT, Kapsimali M, Sumoy L, Goldstone K, Amaya E, Kimelman D, Nicolson T, Gründer S, Gomperts M, Clarke JDW, Wilson SW. 2003. Local tissue interactions across the dorsal midline of the forebrain establish CNS laterality. *Neuron* 39:423–438.
- Cooper MS, D'Amico LA, Henry CA. 1999. Confocal microscopy analysis of morphogenetic movements. *Methods Cell Biol* 59:179–204.
- Dubertret B, Skourides P, Norris DJ, Noireaux V, Brivanlou AH, Libchaber A. 2002. In vivo imaging of quantum dots encapsulated in phospholipid micelles. *Science* 298:1759–1762.
- Dynes JL, Ngai J. 1998. Pathfinding of olfactory neuron axons to stereotyped glomerular targets revealed by dynamic imaging in living zebrafish embryos. *Neuron* 20:1081–1091.
- Fraser SE. 1996. Iontophoretic dye labeling of embryonic cells. *Methods Cell Biol* 51:147–160.
- Gan WB, Grutzendler J, Wong WT, Wong RO, Lichtman JW. 2000. Multicolor “Dioleistic” labeling of the nervous system using lipophilic dye combinations. *Neuron* 27:219–225.
- Gao X, Cui Y, Levenson RM, Chung LWK, Nie S. 2004. In vivo cancer targeting and imaging with semiconductor quantum dots. *Nat Biotechnol* 22:969–976.
- Gitler AD, Lu MM, Epstein JA. 2004. Plexin-D1 and semaphorin signaling are required in endothelial cells for cardiovascular development. *Dev Cell* 7:107–116.
- Gu C, Yoshida Y, Livet J, Reimert DV, Mann F, Merte J, Henderson CE, Jessell TM, Kolodkin AL, Ginty DD. 2005. Semaphorin 3E and Plexin-D1 control vascular pattern independently of neuropilins. *Science* 307:265–268.
- Henry CA, Hall LA, Hille MB, Solnica-Krezel L, Cooper MS. 2000. Somites in zebrafish doubly mutant for *knypek* and *trilobite* form without internal mesenchymal cells or compaction. *Curr Biol* 10:1063–1066.
- Higashijima S, Hotta Y, Okamoto H. 2000. Visualization of cranial motor neurons in live transgenic zebrafish expressing green fluorescent protein under the control of the *islet-1* promoter/enhancer. *J Neurosci* 20:206–218.
- Hove JR, Köster RW, Frouhar AS, Acevedo-Bolton G, Fraser SE, Gharib M. 2003. Intracardiac fluid forces are an essential epigenetic factor for embryonic cardiogenesis. *Nature* 421:172–177.
- Isogai S, Horiguchi M, Weinstein BM. 2001. The vascular anatomy of the developing zebrafish: an atlas of embryonic and early larval development. *Dev Biol* 230:278–301.
- Jaiswal JK, Mattoussi H, Mauro JM, Simon SM. 2003. Long-term multiple color imaging of live cells using quantum dot bioconjugate. *Nat Biotechnol* 21:47–51.
- Jaiswal JK, Goldman ER, Mattoussi H, Simon SM. 2004. Use of quantum dots for live cell imaging. *Nat Methods* 1:73–78.
- Kanda T, Sullivan KF, Wahl GM. 1998. Histone-GFP fusion enables sensitive analysis of chromosome dynamics in living mammalian cells. *Curr Biol* 8:377–385.
- Kane DA. 1999. Cell cycles and development in the embryonic zebrafish. *Methods Cell Biol* 59:11–26.
- Kawakami K, Takeda H, Kawakami N, Kobayashi M, Matsuda N, Mishina M. 2004. A transposon-mediated gene trap approach identifies developmentally regulated genes in zebrafish. *Dev Cell* 7:133–144.
- Kimmel CB, Ballard WW, Kimmel SR, Uhlmann B, Schilling TF. 1995. Stages of embryonic development of the zebrafish. *Dev Dyn* 203:235–310.
- Köster RW, Fraser SE. 2001a. Direct imaging of in vivo neuronal migration in the developing cerebellum. *Curr Biol* 11:1858–1863.
- Köster RW, Fraser SE. 2001b. Tracing transgene expression in living zebrafish embryos. *Dev Biol* 233:329–346.
- Köster RW, Fraser SE. 2005. Time-lapse microscopy of brain development. In: Detrich HW, Zon LI, editors. *The zebrafish: cellular and developmental biology*. San Diego: Academic Press. p 205–233.
- Lansford R, Bearman G, Fraser SE. 2001. Resolution of multiple green fluorescent protein color variants and dyes using two-photon microscopy and imaging spectroscopy. *J Biomed Optics* 6:311–318.
- Larson DR, Zipfel WR, Williams RM, Clark SW, Bruchez MP, Wise FW, Webb WW. 2003. Water-soluble quantum dots for multiphoton fluorescence imaging in vivo. *Science* 300:1434–1436.
- Lawson ND, Weinstein BM. 2002. In vivo imaging of embryonic vascular development using transgenic zebrafish. *Dev Biol* 248:307–318.
- Long QM, Meng AM, Wang H, Jessen JR, Farrell MJ, Lin S. 1997. GATA-1 expression pattern can be recapitulated in living transgenic zebrafish using GFP reporter gene. *Development* 124:4105–4111.
- Lu X, le Noble F, Yuan L, Jiang Q, de Lafarge B, Sugiyama D, Breant C, Claes F, De Smet F, Thomas J-L, Autiero M, Carmeliet P, Tessier-Lavigne M, Eichmann A. 2004. The netrin receptor UNC5B mediates guidance events controlling morphogenesis of the vascular system. *Nature* 432:179–186.
- Lyons DA, Guy AT, Clarke JDW. 2003. Monitoring neural progenitor fate through multiple rounds of division in an intact vertebrate brain. *Development* 130:3427–3436.
- Mattoussi H, Mauro JM, Goldman ER, Green TM, Anderson GP, Sundar VC, Bawendi MG. 2001. Bioconjugation of highly luminescent colloidal CdSe-ZnS quantum dots with an engineered two-domain recombinant protein. *Physica Status Solidi* 224:277–283.
- Niell CM, Meyer MP, Smith SJ. 2004. In vivo imaging of synapse formation on a growing dendritic arbor. *Nat Neurosci* 7:254–260.
- Parinov S, Kondrichin I, Korzh V, Emelyanov K. 2004. Tol2 transposon-mediated enhancer trap to identify developmentally regulated zebrafish genes in vivo. *Dev Dyn* 231:449–459.
- Park KW, Morrison CM, Sorensen LK, Jones CA, Rao Y, Chien CB, Wu JY, Urness LD, Li DY. 2003. Robo4 is a vascu-

- lar-specific receptor that inhibits endothelial migration. *Dev Biol* 261:251–267.
- Park KW, Crouse D, Lee M, Karnik SK, Sorensen LK, Murphy KJ, Kuo CJ, Li DY. 2004. The axonal attractant Netrin-1 is an angiogenic factor. *Proc Natl Acad Sci U S A* 101:16210–16215.
- Rupp RAW, Snider L, Weintraub H. 1994. *Xenopus* embryos regulate the nuclear-localization of Xmyod. *Genes Dev* 8:1311–1323.
- Stainier DYS, Fouquest B, Chen JN, Warren KS, Weinstein BM, Meiler SE, Mohideen MA, Neuhauss SCF, Solnica-Krezel L, Schier AF, Zwartkruis F, Stemple DL, Malicki J, Driever W, Fishman MC. 1996. Mutations affecting the formation and function of the cardiovascular system in the zebrafish embryo. *Development* 123:285–292.
- Teh C, Chong SW, Korzh V. 2003. DNA delivery into anterior neural tube of zebrafish embryos by electroporation. *Bio-techniques* 35:950–954.
- Torres-Vazquez J, Gitler AD, Fraser SD, Berk JD, Pham VN, Fishman MC, Childs S, Epstein JA, Weinstein BM. 2004. Semaphorin-plexin signaling guides patterning of the developing vasculature. *Dev Cell* 7:117–123.
- Voura EB, Jaiswal JK, Mattoussi H, Simon SM. 2004. Tracking metastatic tumor cell extravasation with quantum dot nanocrystals and fluorescence emission-scanning microscopy. *Nat Med* 10:993–998.
- Wang B, Xiao Y, Ding BB, Zhang N, Yuan X, Gui L, X. QK, Duan S, Chen Z, Rao Y, Geng JG. 2003. Induction of tumor angiogenesis by Slit-Robo signaling and inhibition of cancer growth by blocking Robo activity. *Cancer Cell* 4:19–29.
- Weinstein BM, Stemple DL, Driever WD, Fishman MC. 1995. Gridlock, a localized heritable vascular patterning defect in zebrafish. *Nat Med* 11:1143–1147.
- Westerfield M. 1995. *The zebrafish book*. Eugene, OR: University of Oregon Press.
- Wilson SW, Ross LS, Parret T, Easter SS. 1990. The development of a simple scaffold of axon tracks in the brain of the embryonic zebrafish, *Brachydanio rerio*. *Development* 108:121–145.
- Wu X, Liu H, Liu J, Haley KN, Treadway JA, Larson JP, Ge N, Peale F, Bruchez MP. 2003. Immunofluorescent labeling of cancer marker Her2 and other cellular targets with semiconductor quantum dots. *Nat Biotechnol* 21:41–46.